

Figure S1 Lollipop-style mutation diagrams. Lollipop-diagrams to visualize mutations for (A) TP53, (B) PRKDC, (C) KMT2A, and (D) MYCBP2. The x-axis represents the location of the amino acid mutation sites, and the y-axis represents the number of mutations.

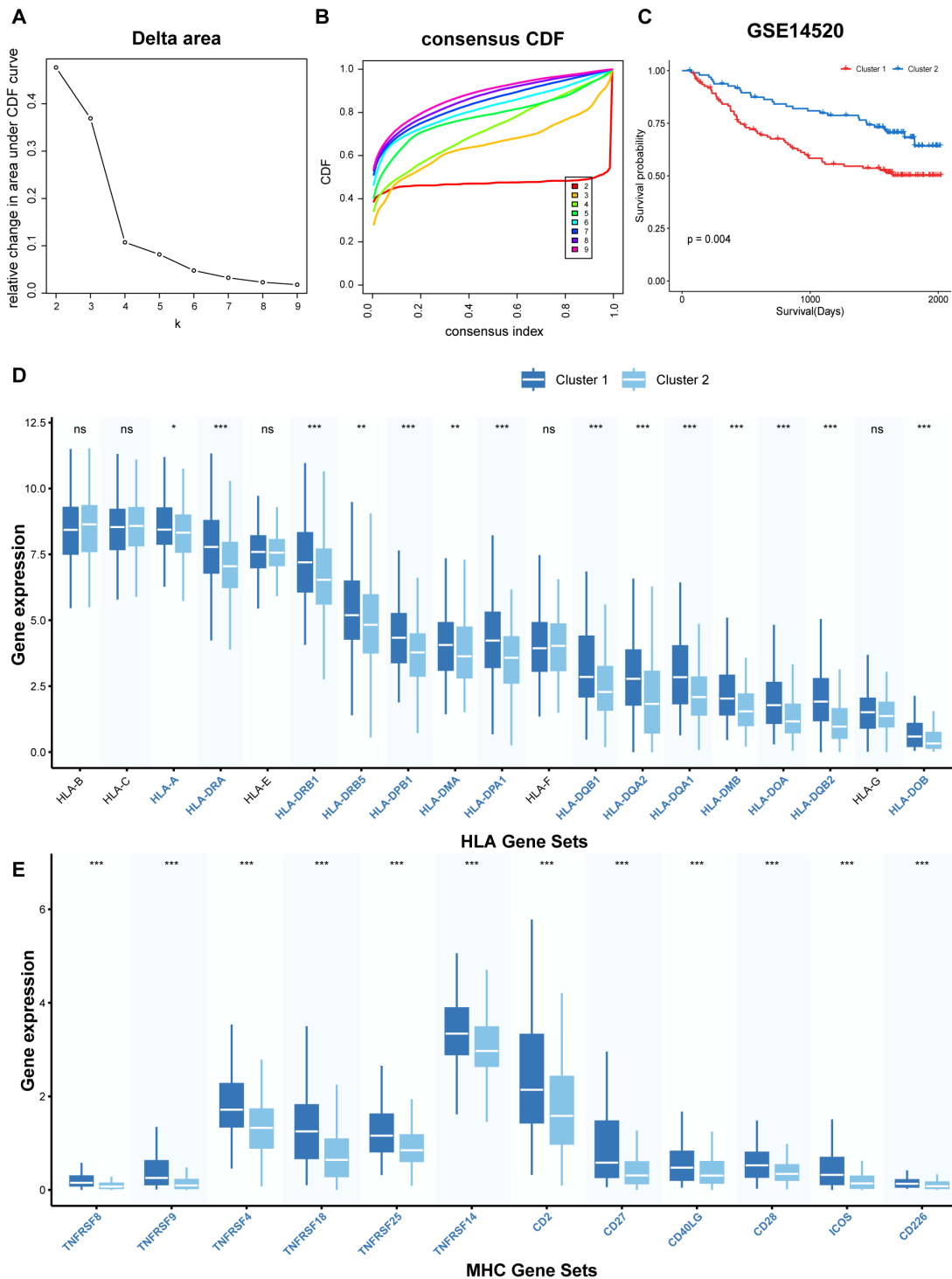


Figure S2 Consensus clustering identified two circadian rhythm-related phenotypes. (A) Relative change in area under CDF curve for $k=2$ to 9. (B) CDF curves of the consensus clustering. (C) The Kaplan-Meier curve of the two circadian rhythm-related phenotypes in GSE14520 via the log-rank test. (D,E) Expression distributions of (D) HLA and (E) MHC gene sets between two circadian rhythm related phenotype clusters. *, $P<0.05$; **, $P<0.01$; ***, $P<0.001$; ns, no statistical significance (Wilcoxon test). HLA, human leukocyte antigen; MHC, major histocompatibility complex; CDF, cumulative distribution function.



B

Gene	HR	lower 95%CI	upper 95%CI	P value
cg01618083	0.000000e+00	0.000	4.578857e+07	0.37
cg02208899	2.405217e+08	102.345	5.652533e+14	0.01
cg12208899	1.431000e+00	0.313	6.533000e+00	0.64
cg15616511	4.040000e-01	0.044	3.664000e+00	0.42
cg20879606	1.000000e-03	0.000	5.673318e+05	0.48
cg21002528	2.310000e-01	0.055	9.690000e-01	0.045
cg21865108	1.093000e+00	0.053	2.257100e+01	0.95
cg22234194	2.509880e+13	11.941	5.275505e+25	0.03
cg23097878	8.620000e-01	0.362	2.051000e+00	0.74
cg24305156	2.223000e+00	0.864	5.724000e+00	0.10
cg24354272	6.770000e-01	0.250	1.836000e+00	0.44
cg24361620	0.000000e+00	0.000	1.342440e+02	0.13
cg24754334	3.362720e+02	0.001	1.197026e+08	0.37
cg26260819	1.681785e+09	0.000	5.083290e+23	0.21
cg26742859	0.000000e+00	0.000	1.178120e+02	0.11
cg27455796	2.122729e+06	0.744	6.055951e+12	0.06

0.5
Hazard ratios

Figure S3 DNA methylation at CpG sites in the *CRY2* gene. (A) *CRY2* methylation map from the MethSurv database. (B) The independent prognosis analysis of CpG sites in *CRY2*. HR, hazard ratio; CI, confidence interval; BMI, body mass index; UCSC, University of California Santa Cruz.

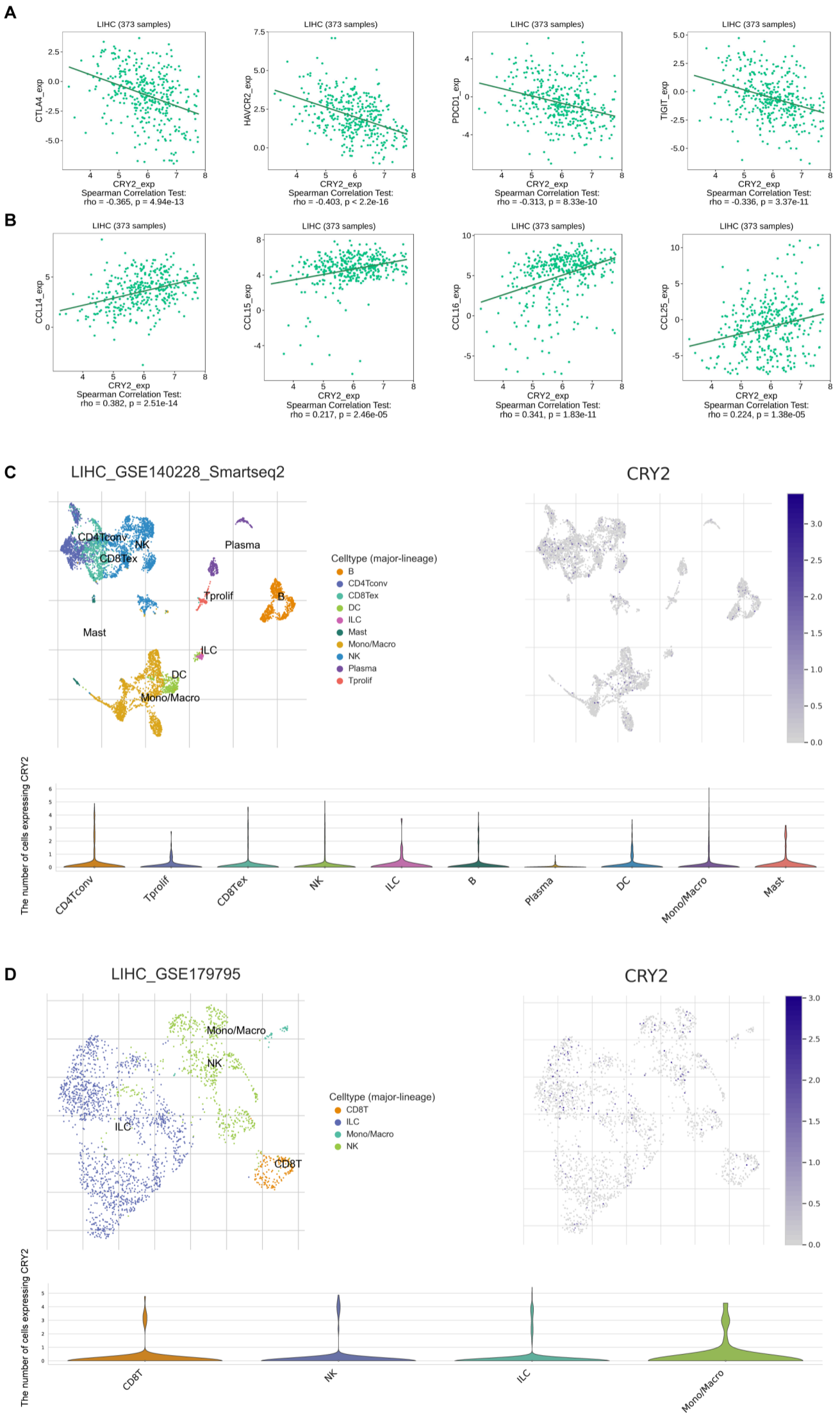


Figure S4 Correlation between CRY2 and tumor immune microenvironment. (A) The association between the expression of CRY2 and immune inhibitors. (B) The association between the expression of CRY2 and chemokines. (C) UMAP plot of 10 major cell clusters in GSE140228_Smartseq2 cohort; The distribution of CRY2 in cell subsets; Violin plot of CRY2 expression at the single cell level. (D) UMAP plot of 4 major cell clusters in GSE179795 cohort; The distribution of CRY2 in cell subsets; Violin plot of CRY2 expression at the single cell level. LIHC, liver hepatocellular carcinoma; CD4Tconv, resting conventional CD4⁺ T cells; CD8Tex, exhausted CD8⁺ T cells; DC, dendritic cell; ILC, innate lymphoid cells; NK, natural killer cell.

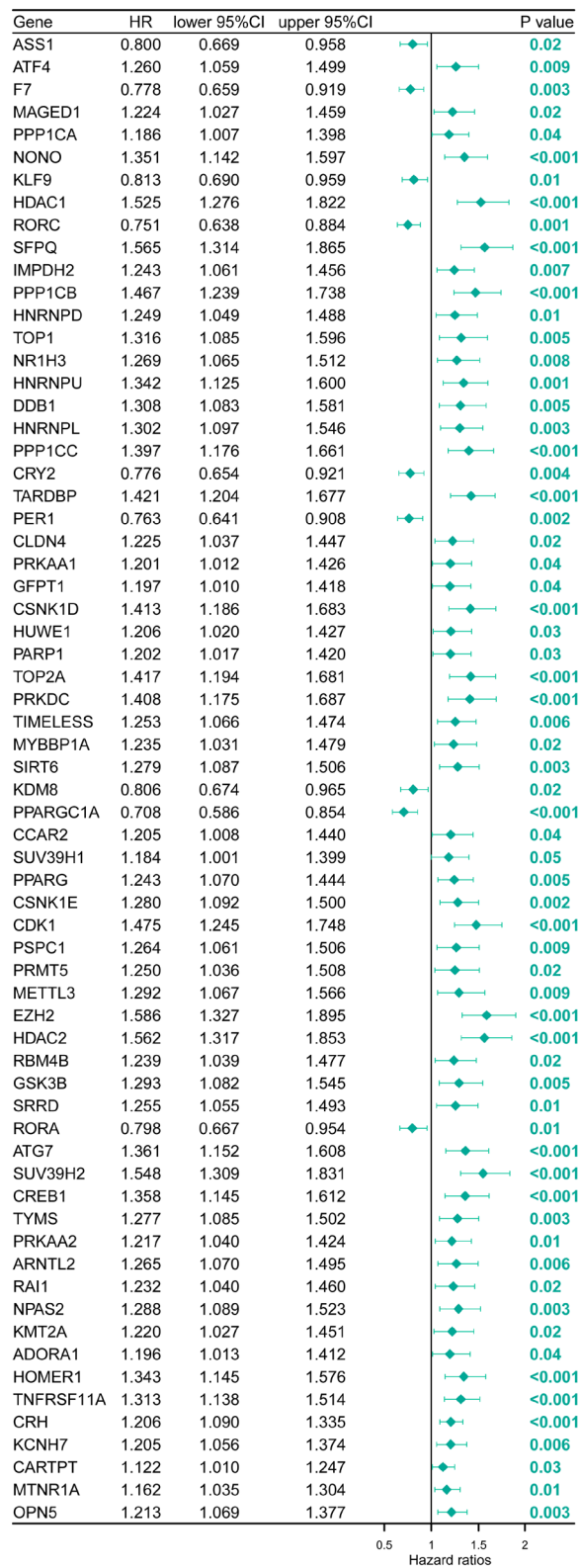


Figure S5 Univariate Cox analysis of 212 CRRGs in TCGA. The forest plot displayed the 66 CRRGs with independent prognosis value in TCGA. TCGA, The Cancer Genome Atlas; CRRGs, circadian rhythm-related genes; HR, hazard ratio; CI, confidence interval.

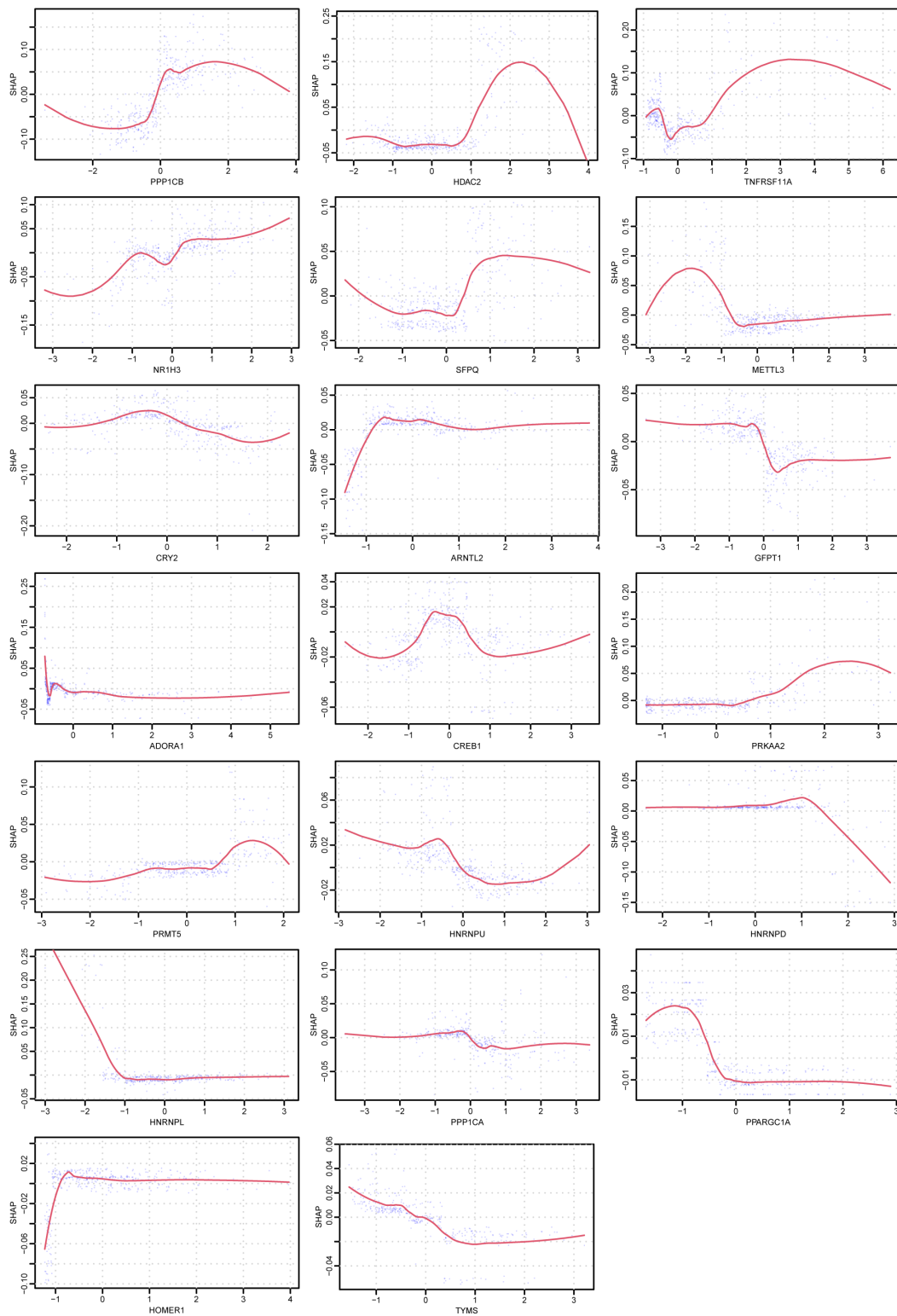


Figure S6 SHAP dependence plot of the XGBoost model. The SHAP dependence plot showed how a single feature could affect the output of the XGBoost prediction model. SHAP values exceeding zero represented that the gene would drive the predictions toward adverse events (higher risk of death). SHAP, SHapley Additive exPlanations; XGBoost, extreme gradient boosting.

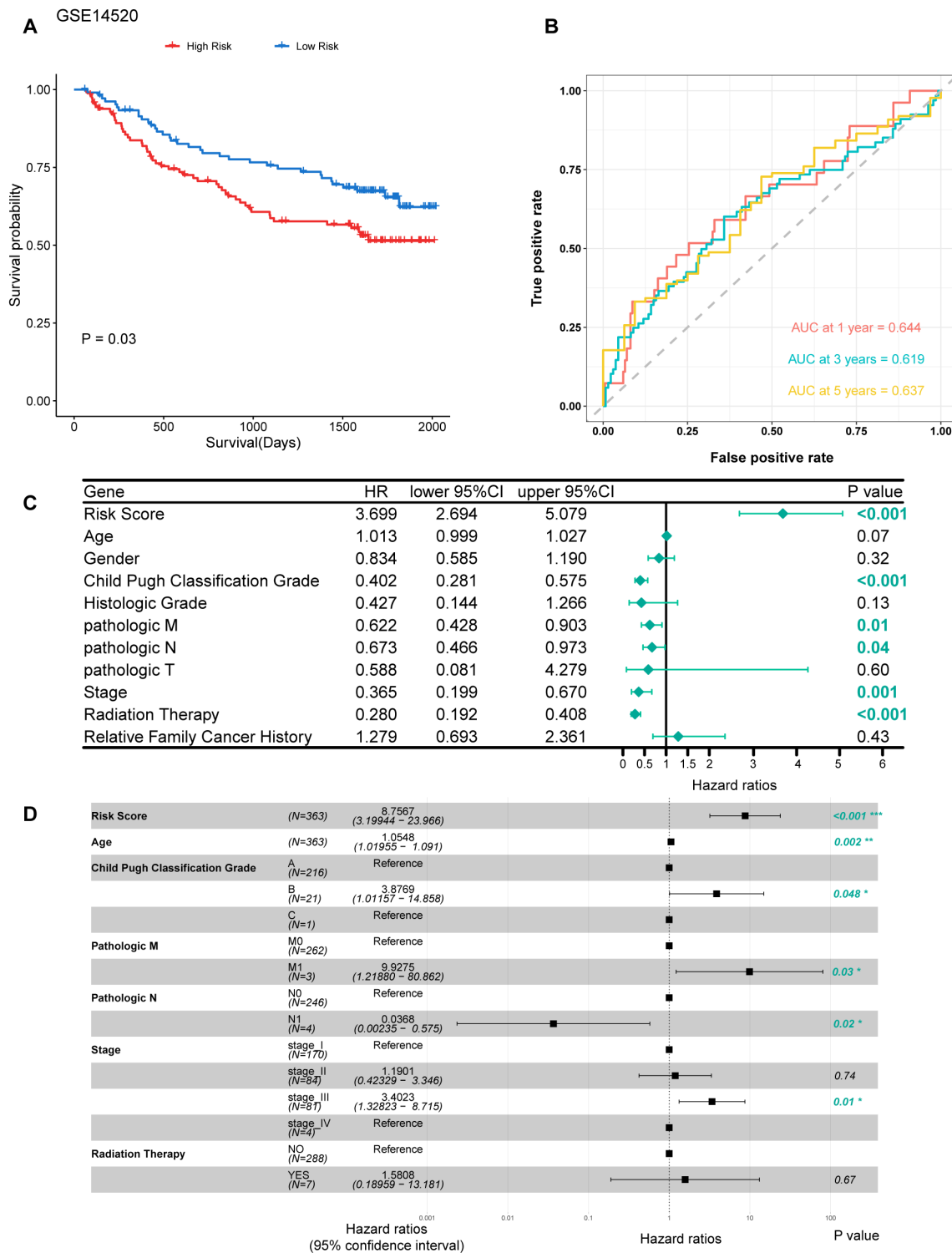


Figure S7 Survival evaluation of CR predictor. (A) Kaplan-Meier curves for OS (log-rank test) in the external validation dataset (GSE14520). (B) Time-dependent ROC curves in the external validation dataset (GSE14520). (C) Univariate and (D) Multivariate Cox analysis containing the CR predictor (risk score) and clinical traits in TCGA. *, $P < 0.05$; **, $P < 0.01$; ***, $P < 0.001$. CR, circadian rhythm; OS, overall survival; ROC, receiver operating characteristic; TCGA, The Cancer Genome Atlas; HR, hazard ratio; CI, confidence interval; AUC, area under the curve.

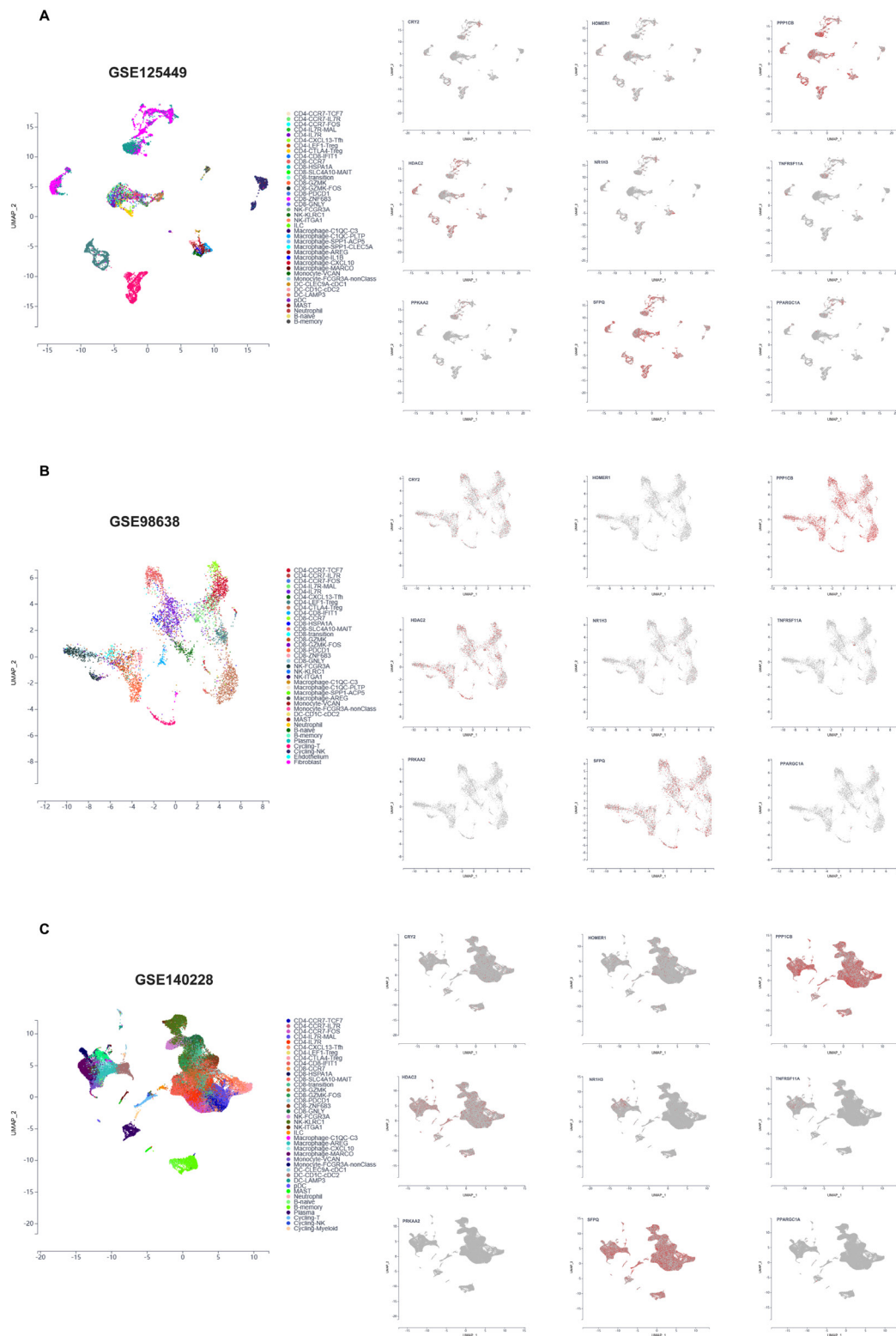


Figure S8 The distribution of model genes within HCC immune microenvironment. UMAP plot of immune cell clusters and the distribution of model genes from (A-C) GSE125449, GSE98638 and GSE140228. HCC, hepatocellular carcinoma; DC, dendritic cell; ILC, innate lymphoid cells; NK, natural killer cell; UMAP, uniform manifold approximation and projection.

Table S1 The SNPs used as genetic instruments in the mendelian randomization analyses for the exposure of genes in CR predictor

Exposure	SNP	Chr	Pos	Effect allele	Other allele	Beta	SE	P	F statistics
NR1H3	rs17725808	11	46444458	C	T	0.188007	0.0348652	6.95E-08	29.08
NR1H3	rs7395581	11	47246397	A	G	0.530587	0.012	1.00E-200	1954.89
NR1H3	rs74390551	11	47407161	T	C	1.22677	0.0332155	1.00E-200	1363.99
NR1H3	rs34874765	11	46565407	A	G	-0.33365	0.0426171	4.92E-15	61.29
NR1H3	rs140745184	11	46942241	T	C	0.223734	0.0344588	8.44E-11	42.15
NR1H3	rs111927021	11	47211568	A	G	-0.107334	0.0138433	8.93E-15	60.11
NR1H3	rs139014611	11	47389687	T	C	0.260607	0.0493461	1.28E-07	27.89
NR1H3	rs188486446	11	46309302	A	G	-0.210181	0.044945	2.92E-06	21.86
NR1H3	rs117082751	11	46572918	A	G	0.231188	0.037945	1.11E-09	37.12
NR1H3	rs11065987	12	112072424	G	A	0.0663553	0.0122449	6.00E-08	29.36
PPARGC1A	rs112951849	4	23833915	G	T	-0.209337	0.0370902	1.66E-08	31.85
PPARGC1A	rs17790469	4	24064757	G	T	0.22321	0.0419512	1.03E-07	28.31
PPARGC1A	rs13108219	4	23908890	A	C	-0.251551	0.017809	2.66E-45	199.50
PPARGC1A	rs189344117	4	24235603	C	T	0.42349	0.0365116	4.19E-31	134.52
PPARGC1A	rs73097695	4	23875401	G	T	0.262996	0.0285366	3.08E-20	84.93
PPARGC1A	rs77983699	4	23885595	C	T	-0.208315	0.0351303	3.03E-09	35.16
PPARGC1A	rs79936066	4	23889124	A	G	-0.275103	0.0335405	2.36E-16	67.27
PPARGC1A	rs61795008	4	23199627	C	T	0.0859621	0.014576	3.69E-09	34.78
PPARGC1A	rs11941854	4	23858960	A	T	0.691899	0.0137137	1.00E-200	2545.35
PPARGC1A	rs646314	4	24043324	C	T	-0.135549	0.0148453	6.80E-20	83.37
PPARGC1A	rs10938987	4	24264014	G	A	0.079775	0.0120508	3.59E-11	43.82
PPARGC1A	rs61196244	4	23801790	C	T	0.169074	0.0298343	1.45E-08	32.11
PPARGC1A	rs7667379	4	24289815	C	T	0.059623	0.0119215	5.70E-07	25.01
PPARGC1A	rs28735003	4	24316054	C	T	0.106144	0.0152606	3.52E-12	48.37
PPARGC1A	rs4917014	7	50305863	G	T	-0.0595623	0.0127871	3.19E-06	21.70
PPARGC1A	rs17694108	19	33731551	A	G	0.0615196	0.0132232	3.28E-06	21.64
CRY2	rs145748086	11	45106271	T	C	0.258926	0.0512278	4.32E-07	25.54
CRY2	rs112259193	11	45157536	T	C	0.277383	0.0420238	4.10E-11	43.56
CRY2	rs2002244	11	45855745	T	C	-0.557661	0.0137378	1.00E-200	1647.68
CRY2	rs2292910	11	45903613	C	A	-0.114339	0.012501	5.90E-20	83.65
CRY2	rs143956160	11	46038617	A	G	0.239904	0.0320736	7.45E-14	55.94
CRY2	rs142583473	11	45933775	T	C	-0.323515	0.0457245	1.49E-12	50.05
CRY2	rs3929339	11	46086727	A	G	-0.193322	0.0190999	4.44E-24	102.44
CRY2	rs7119605	11	45228340	G	A	-0.0747716	0.0119807	4.34E-10	38.95
CRY2	rs4755998	11	45520962	C	T	-0.0660457	0.0138938	2.00E-06	22.60
TNFRSF11A	rs4848370	2	111811665	T	C	-0.0899508	0.0133943	1.87E-11	45.10
TNFRSF11A	rs7911264	10	94436851	C	T	-0.066086	0.011896	2.77E-08	30.86
TNFRSF11A	rs7234211	18	59990831	C	T	-0.133319	0.0133917	2.39E-23	99.10
HDAC2	rs9481408	6	114265287	T	C	-0.0649678	0.0128324	4.13E-07	25.63
HDAC2	rs730445	6	113580669	G	C	0.0792125	0.0157233	4.71E-07	25.38
PPP1CB	rs144683494	2	28755403	C	A	0.207965	0.0434002	1.65E-06	22.96
PPP1CB	rs149532888	2	28999943	G	A	0.345296	0.0448326	1.34E-14	59.31
PPP1CB	rs11676763	2	29208656	T	C	-0.161001	0.0137194	8.39E-32	137.71
PPP1CB	rs7608461	2	29275685	T	C	-0.158227	0.0148713	1.95E-26	113.20
PPP1CB	rs62131773	2	29664491	A	G	-0.100778	0.0202814	6.73E-07	24.69
PPP1CB	rs10171628	2	28819603	T	C	0.134967	0.0139878	4.96E-22	93.10
PPP1CB	rs35720543	2	28832437	G	A	0.251561	0.0191051	1.36E-39	173.36
PPP1CB	rs72790269	2	29473457	A	G	0.16313	0.0295982	3.56E-08	30.37
PPP1CB	rs7586405	2	28906644	G	A	0.558262	0.0120003	1.00E-200	2164.03
PPP1CB	rs62131966	2	29018349	G	A	0.434873	0.0432305	8.37E-24	101.18
PPP1CB	rs112223084	2	29065597	C	T	0.506741	0.035436	2.18E-46	204.48
PPP1CB	rs112452311	2	28789988	A	G	-0.159707	0.0316026	4.34E-07	25.54
PPP1CB	rs113438683	2	28799969	A	G	0.242772	0.0393568	6.90E-10	38.05
PPP1CB	rs114242416	2	29065610	C	T	0.349027	0.0341979	1.86E-24	104.16
PPP1CB	rs6724450	2	29180115	A	G	-0.356329	0.0166173	5.26E-102	459.78
PPP1CB	rs114193888	2	29285987	A	G	-0.251509	0.040085	3.51E-10	39.37
PPP1CB	rs149110519	6	144385777	T	C	0.122185	0.0266379	4.50E-06	21.04

SNPs, single nucleotide polymorphisms; Chr, chromosome; Pos, position; SE, standard error.

Table S2 Results of mendelian randomization analyses

Exposure	Outcome	Method	Number of IVs	P value	OR	95% CIs
NR1H3	HCC	IVW	10	0.280484	0.889066	(0.718113, 1.100716)
PPARGC1A		IVW	16	0.028163	1.285826	(1.027282, 1.60944)
CRY2		IVW	9	0.412477	1.165686	(0.80788, 1.681962)
TNFRSF11A		IVW	3	0.545887	1.366795	(0.495786, 3.76801)
HDAC2		IVW	2	0.545035	0.467541	(0.039859, 5.484182)
PPP1CB		IVW	17	0.426274	1.097434	(0.872775, 1.379921)

IVs, instrumental variables; OR, odd ratio; CI, confidence interval; HCC, hepatocellular carcinoma; IVW, inverse-variance weighted.

Table S3 Sensitivity analysis of mendelian randomization

Exposure	Outcome	Heterogeneity		Pleiotropy		
		Cochran's Q statistic	P value	MR-Egger intercept	SE	P value
NR1H3	HCC	7.31	0.60	-0.04	0.06	0.59
PPARGC1A		12.19	0.66	-0.04	0.04	0.30
CRY2		12.21	0.14	-0.02	0.08	0.83
TNFRSF11A		1.42	0.49	0.11	0.18	0.67
HDAC2		1.53	0.22	NA	NA	NA
PPP1CB		15.12	0.52	-0.02	0.07	0.77

SE, standard error; HCC, hepatocellular carcinoma; NA, not available.

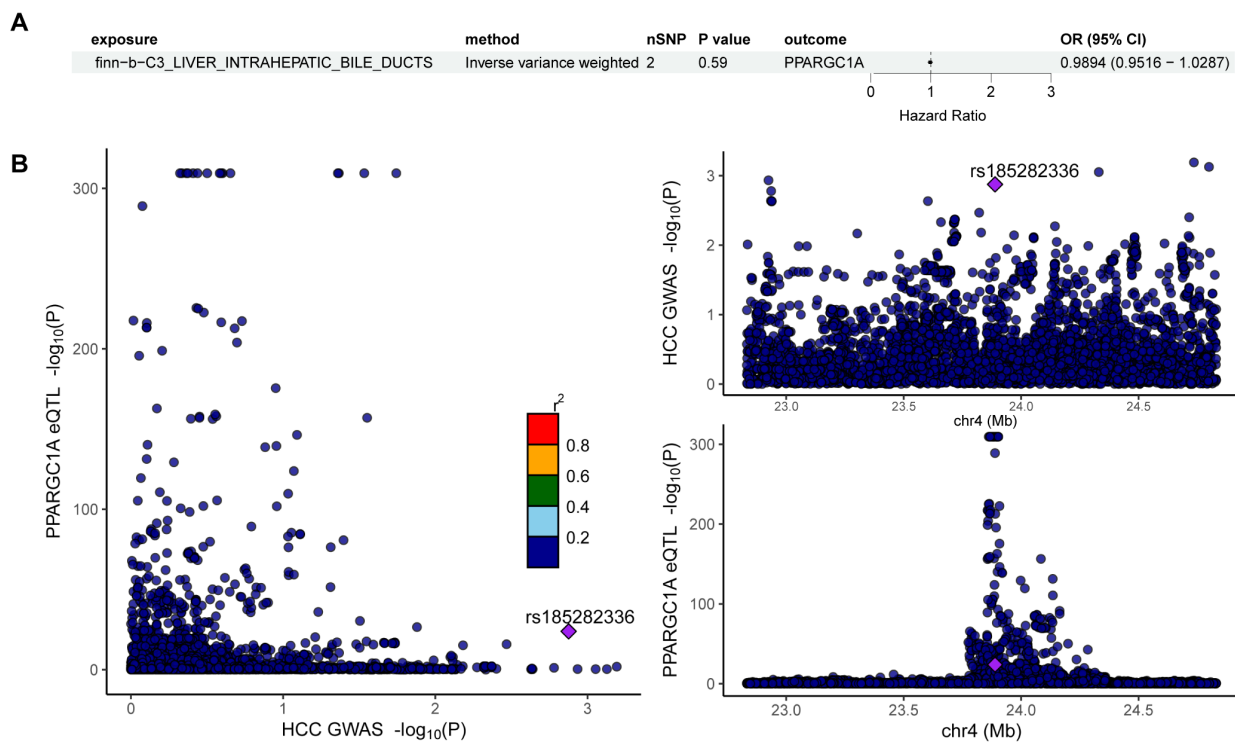


Figure S9 Result of reverse mendelian randomization and colocalization analysis. (A) Causal effects of HCC on PPARGC1A via reverse MR analyses. (B) Colocalization analysis for HCC and PPARGC1A. Association plot showing genome-wide significant loci for HCC in the PPARGC1A gene regions. HCC, hepatocellular carcinoma; MR, Mendelian randomization; nSNP, number of single nucleotide polymorphism; OR, odds ratio; CI, confidence interval; GWAS, Genome-Wide Association Studies; eQTL, expression quantitative trait locus; Chr, chromosome.